Dynamic Obstacle Avoidance with Simultaneous Translational and Rotational Motion Control for Autonomous Mobile Robot

Masaki Takahashi, Takafumi Suzuki, Tetsuya Matsumura, and Ayanori Yorozu

Dept. of System Design Engineering,
Keio University
3-14-1 Hiyoshi, Kohoku-ku, Yokohama 223-8522, Japan
takahashi@sd.keio.ac.jp

Abstract. This paper presents a real-time collision avoidance method with simultaneous control of both translational and rotational motion with consideration of a robot width for an autonomous omni-directional mobile robot. In the method, to take into consideration the robot's size, a wide robot is regarded as a capsule-shaped case not a circle. With the proposed method, the wide robot can decide the direction of translational motion to avoid obstacles safely. In addition, the robot can decide the direction of the rotational motion in real time according to the situation to perform smooth motion. As an example of design method of the proposed method, novel control method based on the fuzzy potential method is proposed. To verify its effectiveness, several experiments using a real robot are carried out.

Keywords: Service Robot, Obstacle Avoidance, Omni-directional Platform, Fuzzy Potential Method.

1 Introduction

Various obstacle avoidance methods and their availabilities for mobile robots have described [1]-[8]. Most of these studies regard the robots as points or circles and discuss control methods of translational motion. In these studies, a non-circle robot is regarded as a circle robot with consideration of maximum size of the robot. The effectiveness of avoiding obstacles by this approach has been confirmed. However, depending on the shape of the robot, this approach reduces and wastes available free space and can decrease the possibility that the robot reaches the goal. If wide robots, which are horizontally long, are regarded as circles in accordance with conventional approaches, they may not be able to go between two objects due to the largest radius of the robot, even if they ought to be able to go through by using their shortest radius. This suggests the necessity of a suitable orientation angle at the moment of avoidance. Consequently, to enable wide robots to avoid obstacles safely and efficiently, it is necessary to control not only a translational motion but also a rotational motion. In our current research, a wide robot with omni-directional platforms shown in Fig.1 is developed.

J.-L. Ferrier et al. (Eds.): Informatics in Control, Automation and Robotics, LNEE 174, pp. 51–64.
springerlink.com

Fig. 1. An autonomous robot for hospital use

Several studies have focused on the orientation angle of the robot [9]; [10]. In these studies, by convolving the robot and the obstacle at every orientation and constructing the C-space, the suitable orientation angles of the robot for path planning are decided. However, these methods require an environmental map and the studies have not shown the effectiveness for avoidance of unknown obstacles by autonomous mobile robots. Therefore, to avoid unknown obstacles reactively with consideration of the orientation angle, wide robots need an algorithm that can decide the orientation angle and rotational velocity command in real time based on current obstacle information.

This study proposes a control method of both translational and rotational motion with consideration of a robot width in order to achieve a smooth motion. With the proposed method, the orientation angle is controlled easily in real time. To verify the effectiveness of the proposed method, several simulations were carried out [11]. In this study, several experiments using our robot shown in Fig.1 are carried out.

2 Simultaneous Translational and Rotational Motion Control

2.1 Problem for Solution

There are various non-circle robots. These are vertically long robots, or wide robots. These robots have two arms mounted on a torso with wheels so these robots can be used for mobility, manipulation, whole-body activities, and human-robot interaction [12]; [13]. For these wide robots, conventional obstacle avoidance methods are incompatible because they regard the robot as a point or a circle. We are developing a wide robot with a torso, two arms and a head shown in Fig.1. It not only moves indoors but also communicates and interacts with humans through gestures or speech. When the robot opens one or both of its arms slightly, as shown in Fig.2(b), it becomes increasingly difficult to apply conventional obstacle avoidance methods. If these wide robots are regarded as circles in accordance with conventional approaches, it may not be possible for them to go between two obstacles due to the largest radius of the robot, even if they ought to go through by using their shortest radius. In this study, a capsule-shaped case is introduced to make wide robots move smoothly and safely in an environment with obstacles.

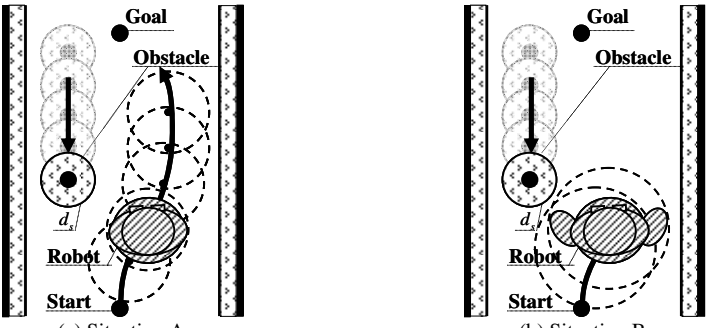

(a) Situation A (b) Situation B

Fig. 2. Two robots which are included in respective circles

2.2 Design of Capsule-Shaped Case

The capsule-shaped case is modeled by two circles and two lines tangent to the circles as shown in Fig.3. This closed contour is defined as $l(\phi)$ with the origin at the point P_O.

$$l(\phi)=\begin{cases} & 0\le\phi<\phi_1 \\ C_a/\cos\phi & if\ \phi_4\le\phi<2\pi \\ -C_a/\cos\phi & if\ \phi_2\le\phi<\phi_3 \\ \sqrt{X(\phi)^2+Y(\phi)^2} & if\ \phi_1\le\phi<\phi_2 \\ & \phi_3\le\phi<\phi_4 \end{cases} \tag{1}$$

where ϕ_i is clockwise from the back direction of the robot.

$$\phi_1=\arctan(C_L/C_a),\ \phi_2=\pi-\arctan(C_L/C_a),$$
$$\phi_3=\pi+\arctan(C_R/C_a),\ \phi_4=2\pi-\arctan(C_R/C_a)$$

$X(\phi)$ and $Y(\phi)$ are calculated as follows.

$$X(\phi)=\begin{cases} \dfrac{-C_L-\sqrt{C_L{}^2-\left(C_L{}^2-C_a{}^2\right)\left\{1+\tan^2(\pi/2-\phi)\right\}}}{1+\tan^2(\pi/2-\phi)} \\ if\quad \phi_1\le\phi<\phi_2 \\ \dfrac{C_R+\sqrt{C_R{}^2-\left(C_R{}^2-C_a{}^2\right)\left\{1+\tan^2(\pi/2-\phi)\right\}}}{1+\tan^2(\pi/2-\phi)} \\ if\quad \phi_3\le\phi<\phi_4 \end{cases} \tag{2}$$

$$Y(\phi)=X(\phi)\tan(\pi/2-\phi) \tag{3}$$

In the proposed method, C_L, C_R ,and C_a are decided in a way that makes wide robot shape fall within the capsule-shaped case.

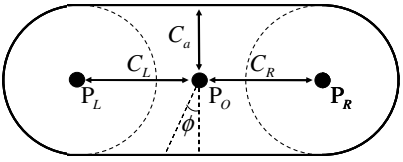

Fig. 3. Capsule-shaped case

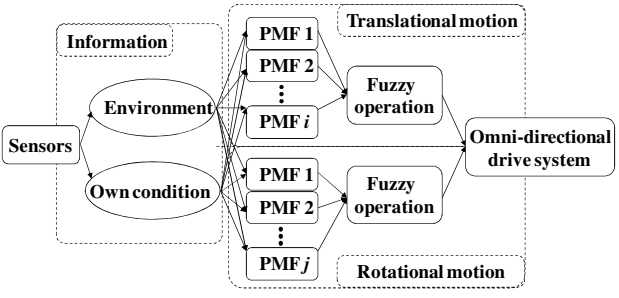

Fig. 4. Concept of fuzzy potential method using both translational and rotational motion with an omni-direction platform

2.3 Controller Design

Figure 4 shows a concept of the fuzzy potential method (FPM) that takes into consideration both translational and rotational motion. In the conventional FPM [14], a command velocity vector that takes into consideration element actions is decided. Element actions are represented as potential membership functions (PMFs), and then they are integrated by means of fuzzy inference. The horizontal axis of PMF is directions which are from $-\pi$ to π radians measured clockwise from the front direction of the robot. The vertical axis of PMF is the grade for the direction. The grade, direction, and configured maximum and minimum speeds, are used to calculate the command velocity vector.

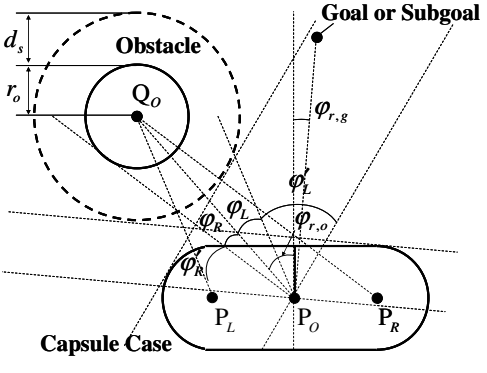

Fig. 5. Wide robot and obstacle

In this research, in addition to conventional approach the PMFs for translational and rotational motion are designed respectively based not only on environmental information but also the robot's condition. Environmental information and the robot's condition are treated separately and divided into a translation problem and a rotational problem. Then the PMFs of each problem are independently integrated using fuzzy inference. Finally, translational and rotational velocity commands, which are calculated by defuzzification of mixed PMFs, are realized by an omni-directional drive system.

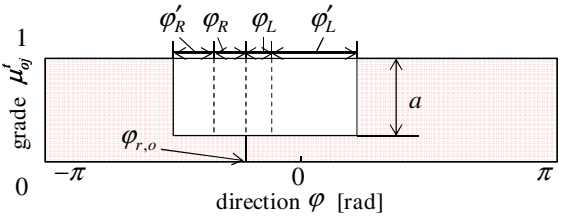

Fig. 6. Example of PMF for an obstacle

2.4 PMF for Translational Motion

2.4.1 PMF for Obstacles

To enable a wide robot to avoid obstacles safely and efficiently in real time, a concave shaped PMF μ^t_{oj} $(j=1,2,\cdots,n)$ shown in Fig.6, which takes into consideration the capsule case, is generated. This PMF is specified by depth and width, which are calculated based on the geometrical relation between an obstacle and the robot as shown in Fig.5. By generating a PMF based on the variables φ_L, φ_R, $\varphi'_L, \varphi'_R, a$ and $\varphi_{r,o}$ in Fig.6, it can choose a safe direction.

$$\varphi_L = \arccos\left(\frac{\left\|\overrightarrow{\mathrm{P}_O\mathrm{Q}_O}\right\|^2 + \left\|\overrightarrow{\mathrm{P}_L\mathrm{Q}_O}\right\|^2 - \left\|\overrightarrow{\mathrm{P}_O\mathrm{P}_L}\right\|^2}{2\left\|\overrightarrow{\mathrm{P}_O\mathrm{Q}_O}\right\| \cdot \left\|\overrightarrow{\mathrm{P}_L\mathrm{Q}_O}\right\|} \right). \tag{4}$$

$$\varphi_R = \arccos\left(\frac{\left\|\overrightarrow{\mathrm{P}_O\mathrm{Q}_O}\right\|^2 + \left\|\overrightarrow{\mathrm{P}_R\mathrm{Q}_O}\right\|^2 - \left\|\overrightarrow{\mathrm{P}_O\mathrm{P}_R}\right\|^2}{2\left\|\overrightarrow{\mathrm{P}_O\mathrm{Q}_O}\right\| \cdot \left\|\overrightarrow{\mathrm{P}_R\mathrm{Q}_O}\right\|} \right). \tag{5}$$

$$\varphi'_L = \begin{cases} \arcsin\left(D \Big/ \left\|\overrightarrow{\mathrm{P}_L\mathrm{Q}_O}\right\| \right) & \text{if } D < \left\|\overrightarrow{\mathrm{P}_L\mathrm{Q}_O}\right\|. \\ \pi - \arcsin\left\{ \left(\left\|\overrightarrow{\mathrm{P}_L\mathrm{Q}_O}\right\| - d_s \right) \Big/ \left(D - d_s \right) \right\} & \text{if } D \geq \left\|\overrightarrow{\mathrm{P}_L\mathrm{Q}_O}\right\|. \end{cases} \tag{6}$$

$$\varphi'_R = \begin{cases} \arcsin\left(D \Big/ \left\|\overrightarrow{\mathrm{P}_R\mathrm{Q}_O}\right\| \right) & \text{if } D < \left\|\overrightarrow{\mathrm{P}_R\mathrm{Q}_O}\right\|. \\ \pi - \arcsin\left\{ \left(\left\|\overrightarrow{\mathrm{P}_R\mathrm{Q}_O}\right\| - d_s \right) \Big/ \left(D - d_s \right) \right\} & \text{if } D \geq \left\|\overrightarrow{\mathrm{P}_R\mathrm{Q}_O}\right\|. \end{cases} \tag{7}$$

As a measure to decide how far the robot should depart from the obstacle, a is defined as the depth of the concave PMF.

$$a = \frac{\alpha - \left\| \mathbf{r}_{r,o} \right\|}{\alpha - D} \qquad if \quad \left\| \mathbf{r}_{r,o} \right\| < \alpha \quad . \tag{8}$$

where $\mathbf{r}_{r,o} = (\mathrm{r}_x, \mathrm{r}_y)$ is the current position vector of the obstacle relative to the robot. If the current obstacle position is inside a circle with radius α from the robot position, a PMF for obstacle avoidance is generated. D is decided to ensure a safe distance.

$$D = C_a + r_o + d_s \quad . \tag{9}$$

C_a is the minimum size of the capsule case, r_o and d_s denote respectively the radius of the obstacle and the safe distance. $\varphi_{r,o}$ is the angle of the direction to the obstacle relative to the robot.

$$\varphi_{r,o} = \arctan(\mathrm{r}_y / \mathrm{r}_x) \quad . \tag{10}$$

For safe avoidance, the PMF μ_{oj}^t is generated for all the obstacles that the robot has detected. Then, they are all integrated by calculating the logical product μ_o^t.

$$\mu_o^t = \mu_{o1}^t \wedge \mu_{o2}^t \wedge \cdots \wedge \mu_{oj}^t \quad . \tag{11}$$

By deciding the depth and the base width of the concave PMF μ_o^t is generated.

2.4.2 PMF for a Goal

To head to the goal, a triangular PMF μ_g^t is generated, as shown in Fig.7. μ_g^t is specified by g_a, g_b ,and $\varphi_{r,g}$. As a measure to decide how close to the goal the robot should go, g_a is defined as the height of the triangular PMF. As a measure to decide how much the robot can back away from obstacles, g_b is defined. μ_g^t

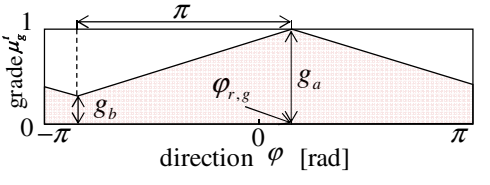

Fig. 7. Example of PMF for a goal

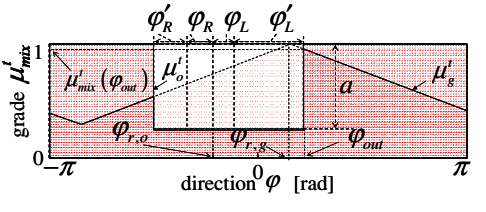

Fig. 8. Example of mixed PMF for translational motion

reaches the maximum value as g_a at an angle of the goal direction relative to the front direction of the robot $\varphi_{r,g}$.

$$g_a = \begin{cases} \dfrac{\left\|\mathbf{r}_{r,g}\right\|}{\varepsilon} & if \quad \left\|\mathbf{r}_{r,g}\right\| \le \varepsilon \\ 1.0 & if \quad \left\|\mathbf{r}_{r,g}\right\| > \varepsilon \end{cases} . \tag{12}$$

$$g_b = \eta g_a \quad (0 \le \eta < 1) . \tag{13}$$

where $\left\|\mathbf{r}_{r,d}\right\|$ is an absolute value of the position vector of the goal relative to the robot. ε and η are constants. If $\left\|\mathbf{r}_{r,d}\right\|$ is below ε, g_a is defined. The robot can decelerate and stop stably.

2.4.3 Calculation of a Translational Command Velocity Vector

The proposed method uses fuzzy inference to calculate the command velocity vector. The PMFs μ_o^t and μ_g^t are integrated by fuzzy operation into a mixed PMF μ_{mix}^t as shown in Fig.8. μ_{mix}^t is an algebraic product of μ_o^t and μ_g^t.

$$\mu_{mix}^t = \mu_g^t \wedge \mu_o^t . \tag{14}$$

By defuzzifier, a velocity command vector is calculated as a traveling direction φ_{out} and an absolute value of the reference speed of the robot based on the mixed PMF μ_{mix}^t. φ_{out} is decided as the direction that makes the PMF $\mu_{mix}^t(\varphi)$ maximum. Based on φ_{out}, v_{out} is calculated as follows.

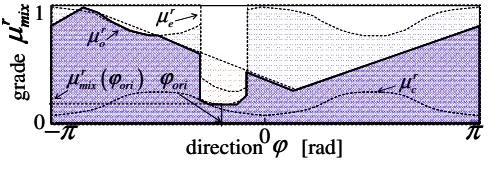

Fig. 9. Example of mixed PMF for rotational motion

$$v_{out} = \mu_{mix}^t(\varphi_{out})(v_{max} - v_{min}) + v_{min} . \tag{15}$$

where $\mu_{mix}^t(\varphi_{out})$ is the mixed PMF for translational motion corresponding to the φ_{out}. v_{max} and v_{min} are respectively the upper and lower limits of the robot speed.

$$\mu_o^r = \mu_e^r - \mu_c^r . \tag{16}$$

2.5 PMF for Rotational Motion

2.5.1 PMF for Obstacles

To enable a wide robot to decide the appropriate angle of the direction for obstacle avoidance in real time, PMF μ_o^r is generated. μ_e^r is generated based on the distance from the center of the robot to obstacles corresponding to all directions, as shown in Fig. 9. The relative distances are obtained with range sensors such as laser range finder, ultra sonic sensors or infrared sensors. μ_c^r is generated based on the capsule case.

$$\mu_c^r(\varphi) = \frac{l(\varphi+\pi)}{\alpha} \quad . \tag{17}$$

The aim of the PMF μ_o^r is to search for an orientation angle of the robot that would maximize the distance between a point on capsule case and each obstacle by turning the front or back side of the robot. By using the capsule case, a PMF design can deal with the width of the robot for rotational motion.

2.5.2 PMF for a Goal

In order to turn the front of the robot toward the goal direction or the travelling direction if there is no obstacle to avoid, PMF for a goal is generated as μ_g^r. This shape is decided in same way as μ_g^t.

2.5.3 Calculation of a Rotational Command Velocity

For the rotational motion, like the translational motion, the rotational command velocity is derived. The PMFs μ_e^r and μ_g^r are integrated by fuzzy operation into a mixed PMF μ_{mix}^r, as shown in Fig.9.

$$\mu_{mix}^r = \mu_g^r \wedge \mu_o^r \quad . \tag{18}$$

By defuzzifier, the command velocity is calculated as a rotational direction φ_{ori} and an absolute value of the reference speed of the robot. φ_{ori} is decided as the direction φ_i that makes the following function $h(\varphi)$ minimum.

$$h(\varphi) = \int_{\varphi-\zeta}^{\varphi+\zeta} \mu_{mix}^r(\psi)\, d\psi \tag{19}$$

where ζ is the parameter to avoid choosing an uncertainty φ_i caused by, for example, noise on the sensor data. On the basis of φ_{ori}, ω is calculated.

$$\omega = \omega_a \,\mathrm{sgn}(\varphi_{ori}) \quad . \tag{20}$$

where ω_a is design variable.

2.6 Omni-Directional Platform

An omni-directional platform was used for the autonomous mobile robot's motion. The command velocity vector was realized by four DC motors and omni wheels.

$$v_r^x = v_{out} \cos \varphi_{out} \quad . \tag{21}$$

$$v_r^y = v_{out} \sin \varphi_{out} \tag{22}$$

where v_{out} and ω are respectively command translational velocity vector and rotational velocity.

$$\begin{bmatrix} v_1^w \\ v_2^w \\ v_3^w \\ v_4^w \end{bmatrix} = \begin{bmatrix} \cos\delta & \sin\delta & R \\ -\cos\delta & \sin\delta & R \\ -\cos\delta & -\sin\delta & R \\ \cos\delta & -\sin\delta & R \end{bmatrix} \begin{bmatrix} v_r^x \\ v_r^y \\ \omega \end{bmatrix} \tag{23}$$

δ is an angle of gradient for each wheel. R is half the distance between two diagonal wheels. v_i^w is a command velocity of each i-th wheel.

Table 1. Parameters in experiments

L	0.4 m	ε	1.0 m	D	0.9 m
C_a	0.3 m	ω_{max}	1.0 rad/s	η	0.2
C_R	0.3 m	W	1.0 m	a_r	1.0 m/s^2
d_s	0.3 m	C_L	0.3 m	ω_{min}	0.0 rad/s
α	4.0 m	r_a	0.3 m		

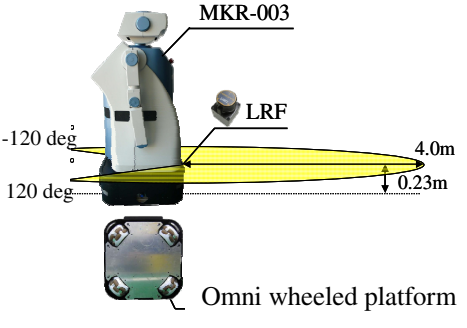

Fig. 10. Laser sensor and an omni-directional platform on an autonomous mobile robot

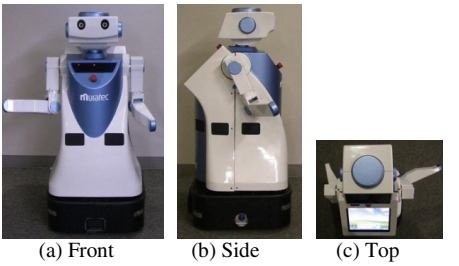

Fig. 11. Experimental situation

3 Experimental Results

3.1 Experimental Condition

To verify the performance of the proposed collision avoidance method to static obstacles, an experiment using the real robot were carried out. In order to recognize the environment, as shown in Fig.10, the robot has external sensors, such as a stereo camera, laser range finder and ultrasonic sensors. However, in this research the robot recognizes the environment using only laser range finder. The upper limit of the velocity of the robot was 0.50 m/s. The upper limit of the acceleration of the robot was 1.0 m/s^2. The arm position was set as shown in Fig.11. Each parameter was shown in Table 1.

3.2 Experimental Results to Static Obstacle

Figure 12 showed that the robot with method I can reach the goal without colliding with the obstacle. However, the position of the right arm comes close to the right-side wall. On the other hand, it was confirmed in Figures 13 and 14 that the robot with the proposed method (method II) changes the orientation angle of the robot to keep the safe distance with the right-side wall and can reach the goal point without colliding with the obstacle.

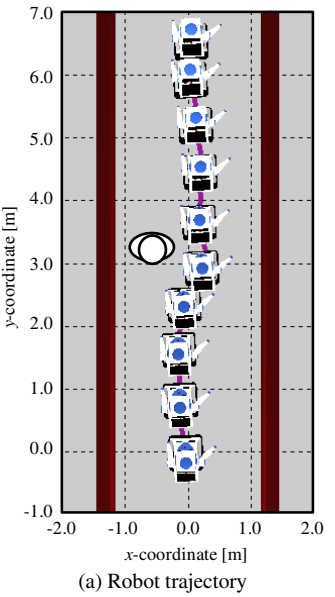

(a) Robot trajectory

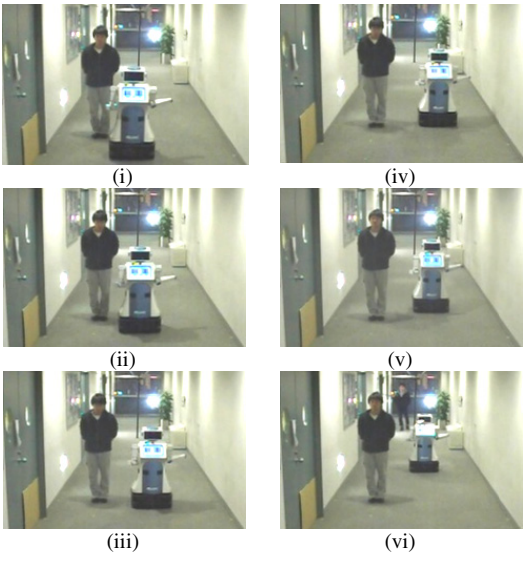

(b) Scenes of the experiment

Fig. 12. Experimental result to static human using fuzzy potential method without PMF for rotational motion (method I)

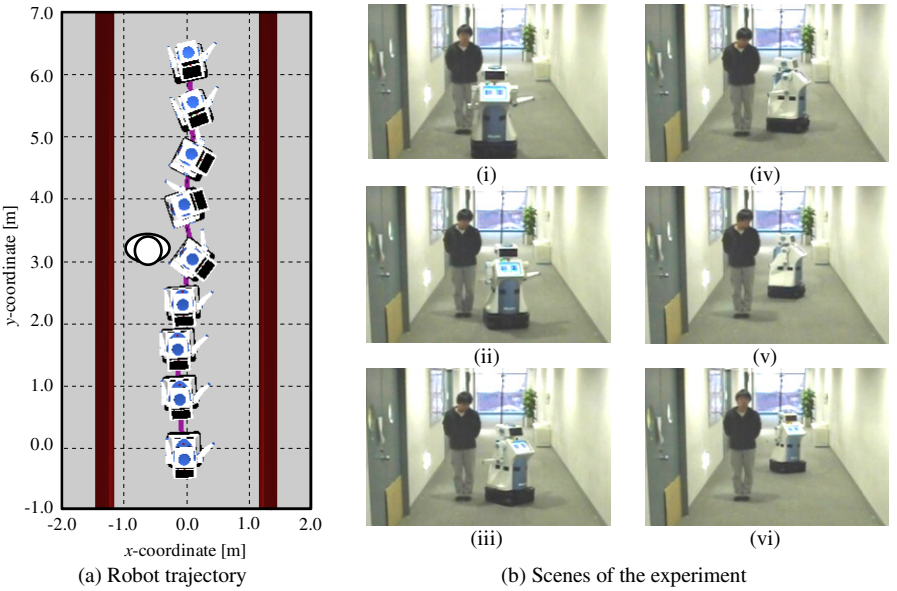

(a) Robot trajectory (b) Scenes of the experiment

Fig. 13. Experimental result to static human using fuzzy potential method with PMF for rotational motion (method II)

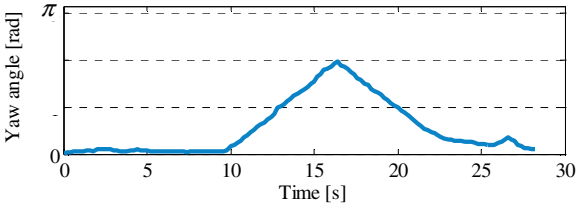

Fig. 14. Time history of yaw angle of the robot

3.3 Experimental Results to Static and Moving Obstacles in Hospital

We carried out the experiments in the hospital. The dish cart was selected as an obstacle. The width of the passage is 2.53 m. The width of the cart is 1.04 m and the depth of the cart is 0.92 m. The safety distance is 0.30 m.

Figure 15 showed the robot trajectory to the static cart using the proposed method. The robot changes the orientation angle of the robot to keep the safe distance with the right-side wall and left-side cart. The minimum distance to the right-side wall was 0.44 m and the minimum distance to the left-side cart was 0.44 m.

Figure 16 showed the robot trajectory to the moving cart using the proposed method. The robot keeps the safe distance with both sides by changing the orientation angle of the robot and can reach the goal point without colliding with the moving cart. However, the robot takes waste motion when the robot closes to the moving obstacle. Therefore, our proposed method should consider the velocity of the obstacle.

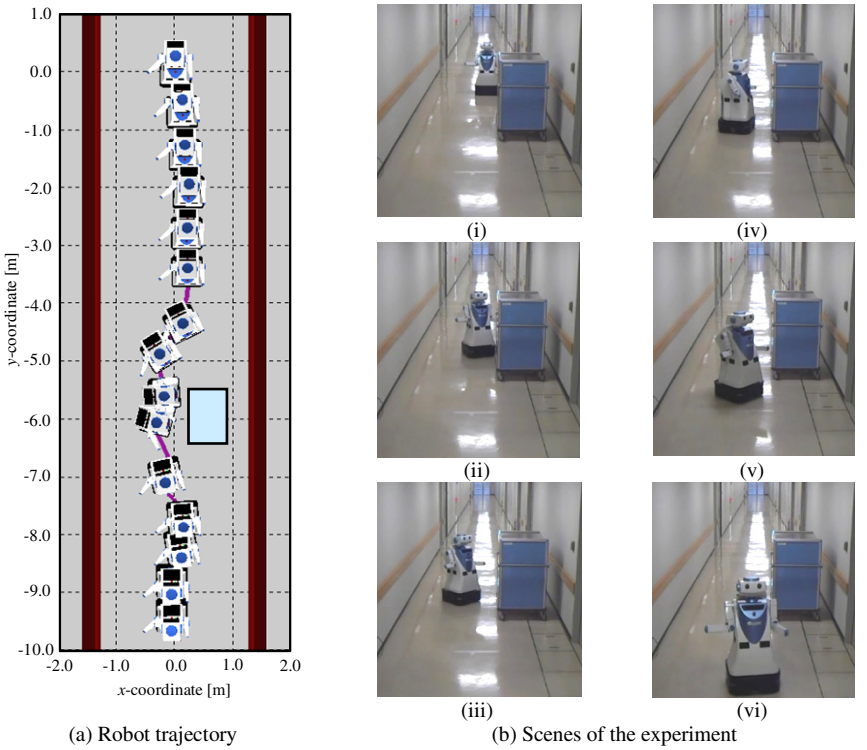

(a) Robot trajectory (b) Scenes of the experiment

Fig. 15. Experimental result to static cart using fuzzy potential method with PMF for rotational motion (method II)

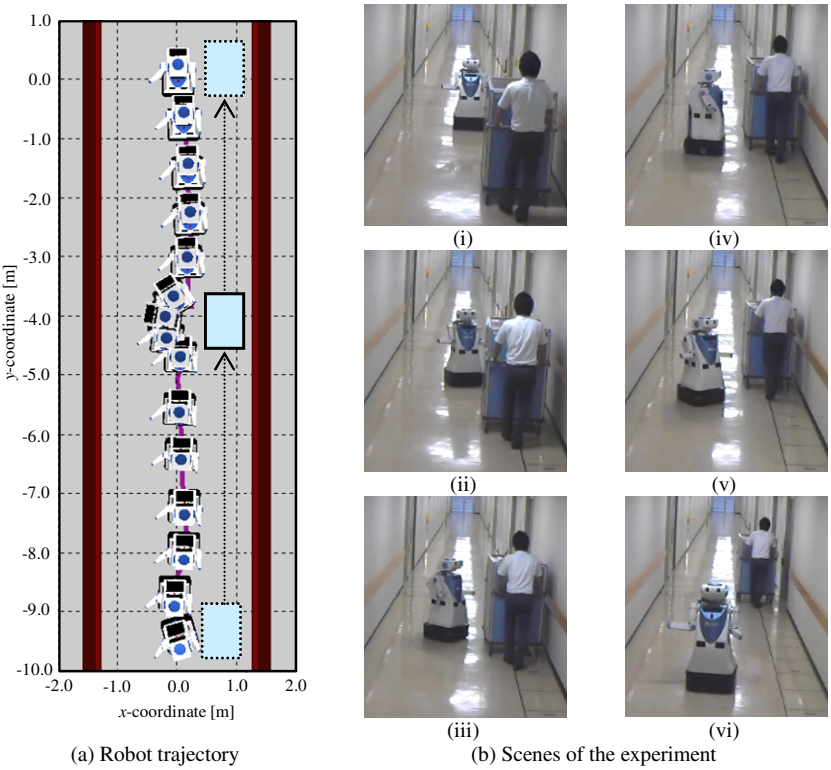

(a) Robot trajectory (b) Scenes of the experiment

Fig. 16. Experimental result to moving cart using fuzzy potential method with PMF for rotational motion (method II)

4 Conclusions

In this paper, the real-time collision avoidance method with simultaneous control of both translational and rotational motion with consideration of a robot width for an autonomous mobile robot, which is horizontally long, has been proposed. This method used an omni-directional platform for the drive system and was based on the fuzzy potential method. The novel design method of potential membership function, which takes the robot's size into consideration using the capsule case, was introduced. With the proposed method, the wide robot can decide the direction of translational motion to avoid obstacles safely. In addition, by controlling rotational motion in real time, the wide robot moves while keeping a safe distance with surroundings in narrow space. The effectiveness has been verified by numerical simulations and experiments. It has been shown that the proposed method performs translational and rotational motion simultaneously according to the situation.

Acknowledgements. This work was supported in part by Grant in Aid for the Global Center of Excellence Program for "Center for Education and Research of Symbiotic, Safe and Secure System Design" from the Ministry of Education, Culture, Sport, and Technology in Japan.

References

1. Du, Z., Qu, D., Yu, F., Xu, D.: A Hybrid Approach for Mobile Robot Path Planning in Dynamic Environments. In: Proc. IEEE Int. Conf. on Robotics and Biomimetics, pp. 1058–1063 (2007)
2. Khatib, O.: Real-time Obstacle Avoidance for Manipulators and Mobile Robots. Int. J. of Robotics Research 5(1), 90–98 (1986)
3. Koren, Y., Borenstein, J.: Potential Field Methods and Their Inherent Limitations for Mobile Robot Navigation. In: Proc. IEEE Int. Conf. on Robotics and Automation, pp. 1398–1404 (1991)
4. Borenstein, J., Koren, Y.: Real-Time Obstacle Avoidance for Fast Mobile Robots. IEEE Trans. on Systems, Man and Cybernetics 19(5), 1179–1187 (1989)
5. Borenstein, J., Koren, Y.: The Vector Field Histogram Fast Obstacle Avoidance for Mobile Robots. IEEE Trans. on Robotics and Automation 7(3), 278–288 (1991)
6. Lumelsky, V.J., Cheung, E.: Real Time Obstacle Collistion Avoidance in Teleoperated Whole Sensitive Robot Arm Manipulators. IEEE Trans. Systems, Man and Cybernetics 23(1), 194–203 (1993)
7. Borenstein, J., Koren, Y.: The Vector Field Histogram Fast Obstacle Avoidance for Mobile Robots. IEEE Trans. on Robotics and Automation 7(3), 278–288 (1991)
8. Dieter, F., Wolfram, B., Sebastian, T.: The Dynamic Window Approach to Collision Avoidance. IEEE Robotics and Automation 4(1), 1–23 (1997)
9. Kavraki, L.: Computation of Configuration Space Obstacles Using the Fast Fourier Transform. IEEE Trans. on Robotics and Automation 11(3), 408–413 (1995)
10. Wang, Y., Chirikjian, G.S.: A New Potential Field Method for Robot Path Planning. In: Proc. IEEE Int. Conf. on Robotics and Automation, San Francisco, CA, pp. 977–982 (2000)
11. Takahashi, M., Suzuki, T., Matsumura, T., Yorozu, A.: Obstacle Avoidance with Simultaneous Translational and Rotational Motion Control for Autonomous Mobile Robot. In: Proc. of the 8th Int. Conf. on Informatics in Control, Automation and Robotics (2011)
12. Ambrose, R.O., Savely, R.T., Goza, S.M., Strawser, P., Diftler, M.A., Spain, I., Radford, N.: Mobile manipulation using NASA's robonaut. In: Proc. IEEE ICRA, pp. 2104–2109 (2004)
13. Takahashi, M., Suzuki, T.: Multi Scale Moving Control Method for Autonomous Omni-directional Mobile Robot. In: Proc. of the 6th Int. Conf. on Informatics in Control, Automation and Robotics (2009)
14. Tsuzaki, R., Yoshida, K.: Motion Control Based on Fuzzy Potential Method for Autonomous Mobile Robot with Omnidirectional Vision. Journal of the Robotics Society of Japan 21(6), 656–662 (2003)